Small Wind Generator System with Non-Inverting Buck-Boost Converter and Battery Storage

Zahari Zarkov[1], Ivan Bachev[2], Vladimir Lazarov[3]

[1] Technical University of Sofia, Faculty of Electrical Engineering, e-mail: zzza@tu-sofia.bg
[2] Technical University of Sofia, French Language Faculty of Electrical Engineering, e-mail: iv.bachev@tu-sofia.bg
[3] Technical University of Sofia, Faculty of Electrical Engineering, e-mail: vl_lazarov@tu-sofia.bg

***Abstract*— A small wind generator system with a claw-pole permanent magnet synchronous generator and a non-inverting buck-boost converter has been modelled in this study. The system uses a battery as a storage device and for stabilization of the output voltage. The system was simulated with four different battery voltages and changing wind speed. The results from the study provide a basis for optimal choice of electrical generator, battery voltage and capacity and give possibility for further development.**

Keywords—small wind generator; PMSG; non-inverting buck-boost converter; MPPT.

I. INTRODUCTION

According to the IEC-61400-2 standard, a small wind generator is a wind turbine with nominal rotor blades swept area of less than 200m^2 and generator voltage of up to 1000VAC or 1500VDC [1]. The definition is further expanded by WWEA. The authors in [2] propose that a small wind turbine uses a generator with nominal electrical power of less than 100kW. In recent years, the number of the installed small wind generators has grown globally. The average power of a small wind generator has increased up to 0.87 kW per unit. In 2014 the cumulative installed power of small wind generators worldwide has reached 830 MW, with the number reaching almost 1 million installed units [2] – Fig. 1 and Fig. 2.

Given this trend, the main goal of this work is to study the behavior of a small wind energy conversion system (WECS) with different battery configurations, which could be used for autonomous consumers. The block diagram of the studied system is shown on Fig. 3.

II. SYSTEM DESCRIPTION

The studied WECS comprises a wind turbine, transmission, permanent magnet synchronous generator, diode rectifier, non-inverting buck-boost converter, lead-acid battery and a load (Fig.3). The choice of a non-controlled diode rectifier working with a DC-DC converter allows for control of the system, compared to the systems that use only diode rectifiers, while at the same time lowering the end price of the whole system, compared to systems with fully controlled rectifiers [3]. The system is modelled in Matlab's Simulink and Simscape environments. The models of the system elements are described below.

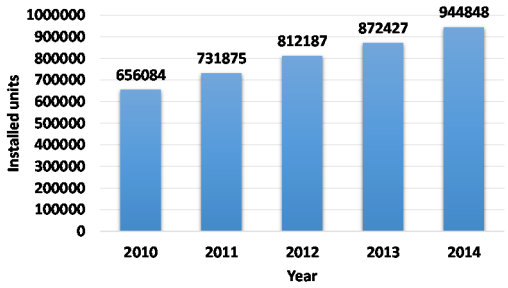

Fig. 1. Small wind generator units installed worldwide [2].

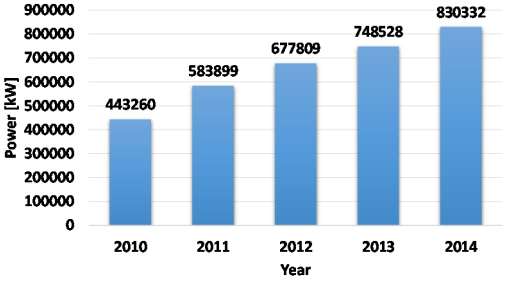

Fig. 2. Cumulative installed power of small wing generators [2].

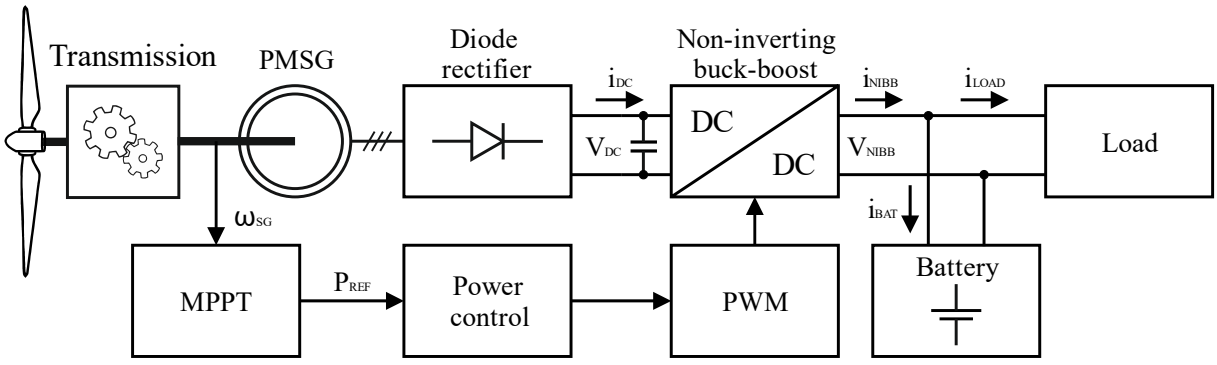

Fig. 3. Configuration of the studied small WECS.

A. Wind Turbine Characteristics

The equations used to model the wind turbine are known from the literature [4]. The wind power extracted by the turbine is:

$$P_{WT} = \frac{1}{2}\rho A v^3 C_p(\lambda,\theta) \tag{1}$$

where ρ is the air density equal to 1.225 kg/m^3, A is the turbine swept area, v is the wind speed, C_p is the turbine power coefficient which depends on the tip speed ratio and θ is the turbine blade pitch angle.

The tip speed ratio (TSR) is defined as:

$$\lambda = \frac{\omega_1 R}{v} \tag{2}$$

where ω_1 is the turbine angular velocity and R is the turbine blade radius.

The pitch regulated turbine power coefficient can be approximated using the following expressions:

$$C_p = a_1\left(\frac{a_2}{\lambda_i} - a_3\theta - a_4\right)e^{\frac{-a_5}{\lambda_i}} \tag{3}$$

$$\frac{1}{\lambda_i} = \left(\frac{1}{\lambda + b_1\theta} - \frac{b_2}{\theta^3+1}\right) \tag{4}$$

Here θ is the pitch angle of the turbine blades and the curve approximating coefficients are a_1=0.08; a_2=100; a_3=0.4; a_4=38; a_5=2.56; b_1=0.08; b_2=0.035.

The wind turbine's power characteristics for different wind speeds and the maximum power curve (MPC) are shown in Fig.4.

B. Transmission

The transmission used in the system is an ideal gear box with a fixed gear ratio of N=25.18. The equation describing the transmission is:

$$\omega_2 = N\omega_1 \tag{5}$$

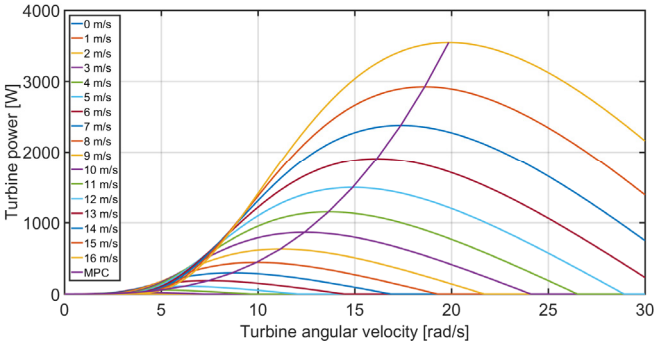

Fig. 4. Power characteristics and MPP curve of the wind turbine for different wind speeds.

where ω_1 is the wind turbine angular velocity, ω_2 is the generator shaft angular velocity and N is the gear ratio.

C. Permanent Magnet Synchronous Generator

The model of the PMSG uses the equations of the generalized theory of the electrical machines [5]. The machine under study is a claw-pole automobile alternator. The alternator was modified by the authors as described in a previous study [6]. The generator's excitation winding has been replaced by a ring-shaped Neodymium magnet – Fig. 5.

The equations describing the generator operation:

$$\begin{cases} \dfrac{d\Psi_d}{dt} = v_d + \omega_r\Psi_q - R_S\dfrac{\Psi_d - L_{pm}i_{pm}}{L_d} \\ \dfrac{d\Psi_q}{dt} = v_q + \omega_r\Psi_d - R_S\dfrac{\Psi_q}{L_q} \end{cases} \tag{6}$$

where v_d and v_q are the stator voltages on the direct and the quadrature axes, R_s is the stator winding resistance, and the permanent magnets are represented by an equivalent inductance L_{pm} and the equivalent magnetizing current i_{pm}, which are referenced to the stator.

The currents in the PMSG can be represented by the flux linkages:

$$\begin{cases} i_d = \dfrac{\Psi_d - L_{pm}i_{pm}}{L_d} \\ i_q = \dfrac{\Psi_q}{L_q} \end{cases} \tag{7}$$

Here i_d and Ψ_d are the projections of the current space vector and the flux linkage space vector on the d axis, i_q and Ψ_q are the projections of the current space vector and the flux linkage space vector on the q axis, L_d and L_q are the stator inductances for the axes d and q.

The equation describing the generator electromagnetic torque is:

$$T_e = \frac{3}{2}p_p\left(L_d - L_q\right)i_d i_q + \frac{3}{2}p_p L_{pm} i_{pm} i_q \tag{8}$$

where T_e is the electromagnetic torque, p_p is the number of pole pairs.

Fig. 5. The modified claw-pole rotor of the generator.

The first term of the equation is the reluctance torque created by the difference of the inductances L_d and L_q and the second term is the torque created by the magnetic field of the permanent magnets.

The drivetrain equation is:

$$\frac{d\omega_2}{dt} J_2 + T_e = \frac{T_{WT}}{N} \tag{9}$$

where T_e is the electromagnetic torque, T_{WT} is the torque of the wind turbine and the moment of inertia J_2 is defined by:

$$J_2 = J_{rotor} + \frac{J_{WT}}{N^2} \tag{10}$$

Here J_{rotor} is the moment of inertia of the electrical generator's rotor and J_{WT} is the moment of inertia of the wind turbine.

D. Diode Rectifier

The rectifier used in this system is represented by a diode rectifier model from the Matlab/Simscape library.

E. Non-inverting Buck-boost Converter

The DC-DC converter used in the system is a non-inverting buck-boost (NIBB) converter [7], [8]. This topology has been chosen because it allows for a wide range of input voltages, thus allowing the generator to work in a wide speed range. The wider range of generator speeds allows for better productivity of the WECS [9]. The NIBB circuit is presented at Fig. 6.

The equations that describe the converter's operation are shown below. When both transistors Q1 and Q2 are ON, the equations for the currents and voltages in the circuit are:

$$\begin{cases} \dfrac{di_L}{dt} = \dfrac{1}{L} V_{DC} \\ \dfrac{dV_{NIBB}}{dt} = \dfrac{1}{C_O}(-i_{NIBB}) \end{cases} \tag{11}$$

where i_L is the current in the inductor, V_{DC} - the input voltage, V_{NIBB} - the output voltage, i_{NIBB} is the output load current, L is the inductance of the converter's inductor and C_O is the capacity of the output capacitor.

When the transistors Q1 and Q2 are OFF the equations become:

$$\begin{cases} \dfrac{di_{L1}}{dt} = \dfrac{1}{L}(-V_{NIBB}) \\ \dfrac{dV_{NIBB}}{dt} = \dfrac{1}{C_O}(i_{L1} - i_{NIBB}) \end{cases} \tag{12}$$

considering that the output voltage is equal to the capacitor voltage $V_{NIBB} = V_{CO}$.

The output voltage dependency on the input voltage and duty ratio D is:

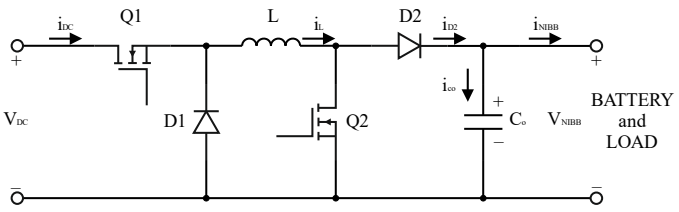

Fig. 6. Non-inverting buck-boost converter.

$$V_{NIBB} = V_{DC}\left(\frac{D}{1-D}\right) \tag{13}$$

F. Control and Maximum Power Point Tracking

The maximum power point tracking (MPPT) algorithm uses a predefined power curve [10]. The maximum power curve of the turbine as a function of the turbine rotational speed for different wind speeds is calculated and is shown on Fig. 4.

The equation approximating the maximum turbine power is:

$$P_M = k\omega_1^3 \tag{14}$$

Here P_M is the maximum available power, and k is a curve fitting coefficient, derived from the turbine's maximum power curve.

The MPPT algorithm uses the generator shaft speed to calculate the wind turbine speed according to (5). Then, the maximum electrical power P_{Gmax} produced by the generator after the rectifier for the current turbine speed is derived

$$P_{G\max} = P_M \eta \tag{14}$$

where η is the generator efficiency, including the rectifier.

The rectifier output current reference is calculated from P_{Gmax} and the measured rectifier voltage V_{DC}:

$$i_{DC-REF} = \frac{P_{G\max}}{V_{DC}} \tag{14}$$

The calculated current value is used as a reference for a PI current controller that regulates the duty ratio of the NIBB converter via PWM block. By changing the pulses' duty ratio the converter adjusts its input current to a value that is necessary to maintain the turbine operating point at the maximum power for the current wind speed. The block diagram of the MPPT algorithm is shown on Fig. 7.

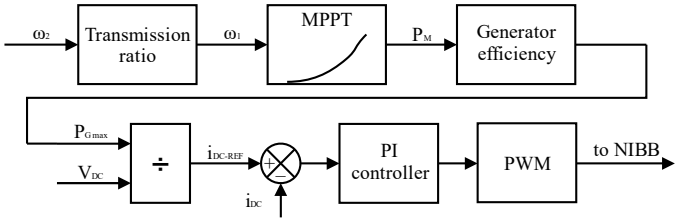

Fig. 7. Block diagram of the MPPT algorithm and power control.

G. Battery

The model of the battery is a finite, charge-dependent voltage source with a series resistance presented in the Matlab/Simscape library. Its voltage has a reciprocal relationship with the charge, defined by the equation:

$$V = V_{FC}\left(1 - \frac{\alpha(1-x)}{1-\beta(1-x)}\right) \quad (15)$$

where x is the ratio of the charge left to the rated or full charge for the battery, V_{FC} is the voltage when the battery is fully charged, α and β are curve-fitting constants.

The batteries used in the study are: 12V – 800Ah, 24V – 400Ah, 36V – 300Ah and 48V – 200Ah, thus allowing for equal energy storage capacity. It must be noted that the 36V system requires 9 pcs. 12V - 100Ah batteries and the other three configurations require 8 pcs. 12V – 100Ah batteries, which difference does not affect much the results.

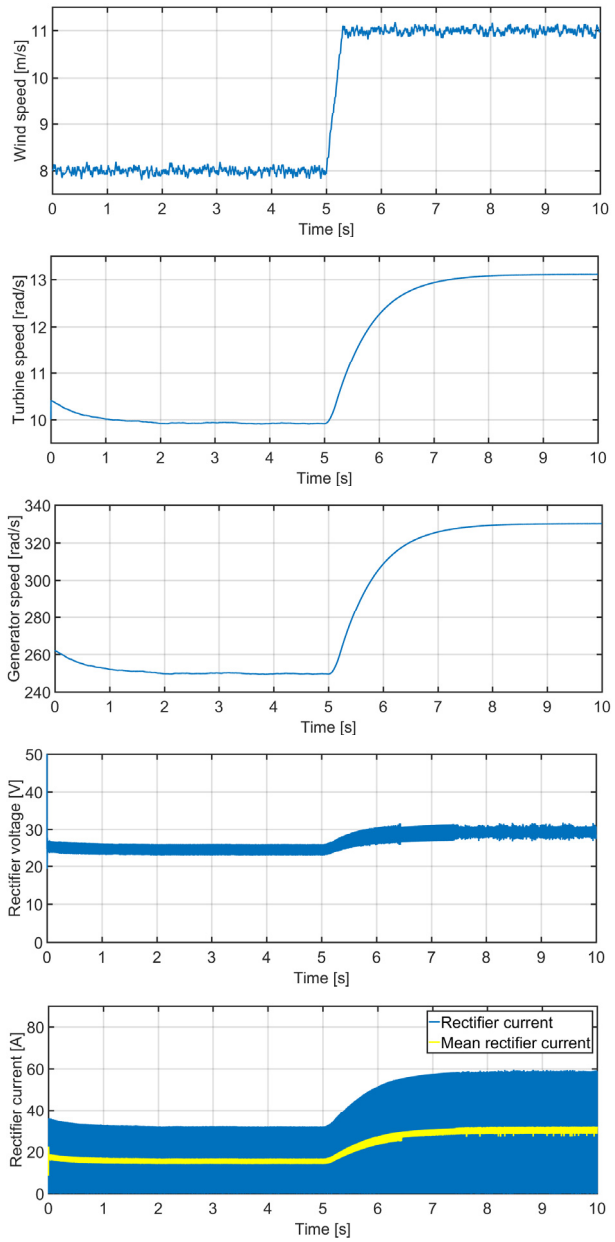

Fig. 8. System behavior at step wind change. From top to bottom: wind speed, turbine speed, generator speed, rectifier voltage and rectifier current.

H. Load

The system load is represented by an equivalent resistance, calculated for total power of 600W at every of the battery voltages 12, 24, 36, and 48V. This value of the power is chosen because it is the rated power of the electrical generator.

III. Study and Results

The studied system was simulated using four different battery voltages as mentioned before. The wind speed profile is

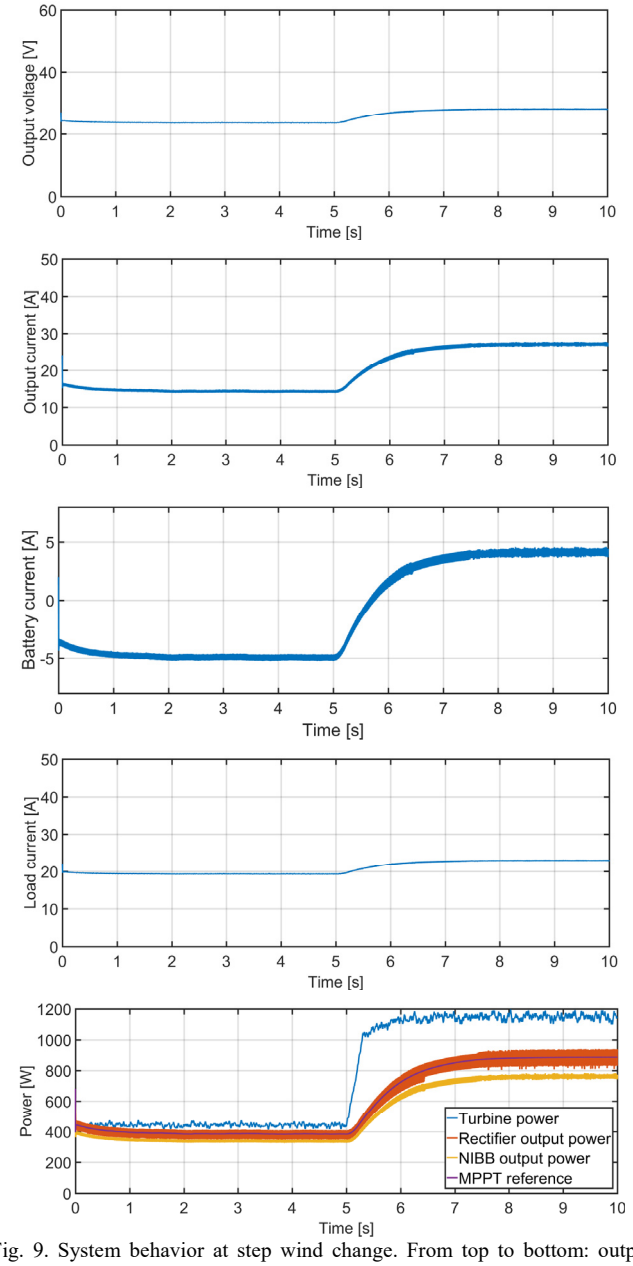

Fig. 9. System behavior at step wind change. From top to bottom: output voltage of the NIBB converter, NIBB output current, battery current, load current and system's power comparison.

the same for all the cases and the load is 600W, represented by an equivalent resistance.

The wind profile is represented in Fig. 8 (top graph). The change in the wind speed from 8 m/s to 11 m/s in the 5th second is used to show the ability of the system to respond to sudden changes.

The different battery voltages impose different working conditions of the NIBB converter. Depending on the output voltage implied by the chosen battery configuration the converter operates in different modes - step-down or step-up. Since there are similarities in the behavior of the simulated systems with different battery voltages, the complete set of results only for the system, using 24V battery is shown in Fig. 8 and Fig. 9. Other systems' results are displayed when appropriate.

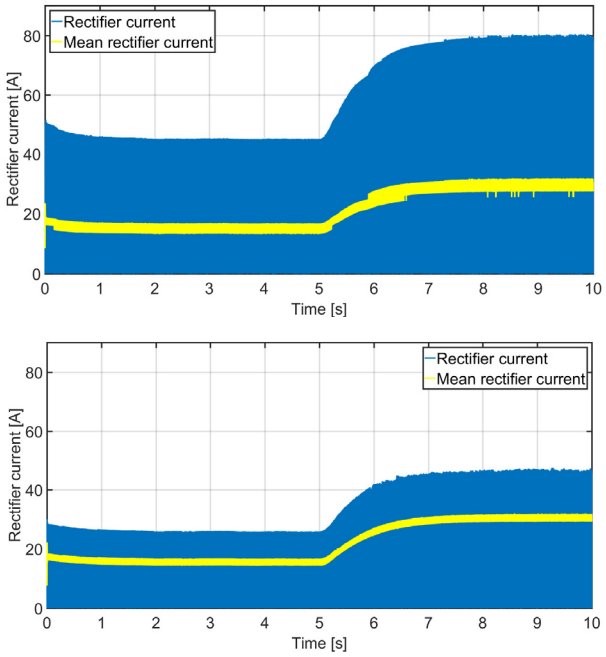

Fig. 10. Output current of the diode rectifier (I_{DR}) for the 12V system (top) and 48V system (bottom).

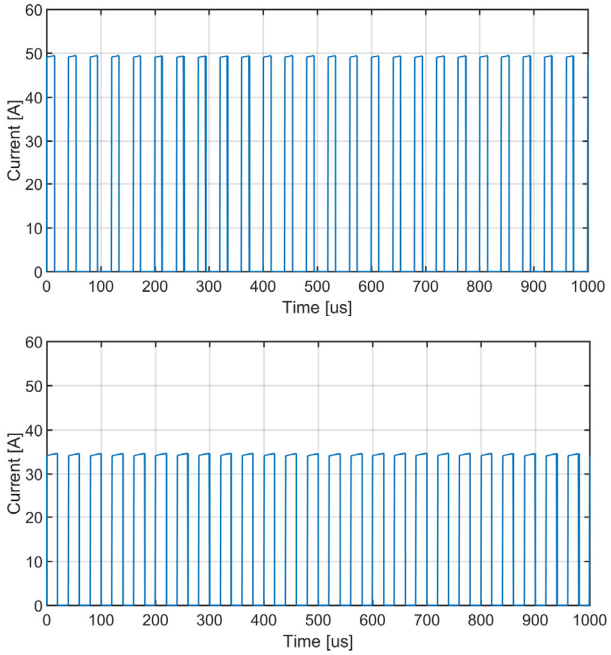

Fig. 11. Zoom-in of the diode rectifier output current (I_{DR}) for the 12V system (top) and 48V system (bottom).

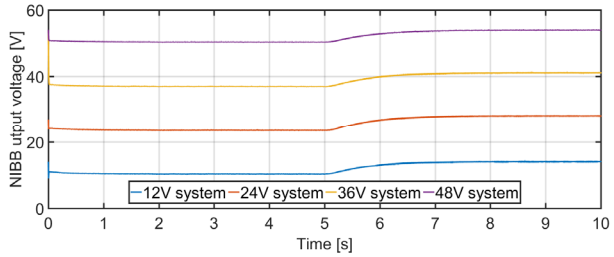

Fig. 12. Comparison of the output voltage of the NIBB converters.

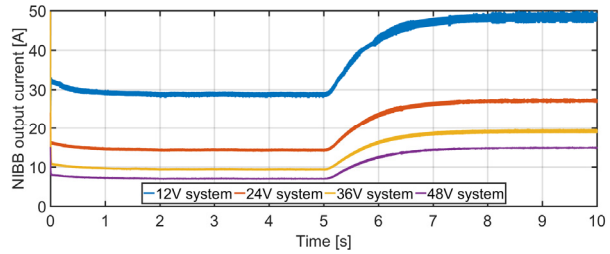

Fig. 13. Comparison of the output current of the NIBB converters.

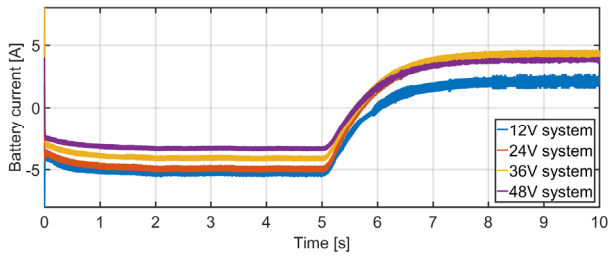

Fig. 14. Battery curent for the four cases.

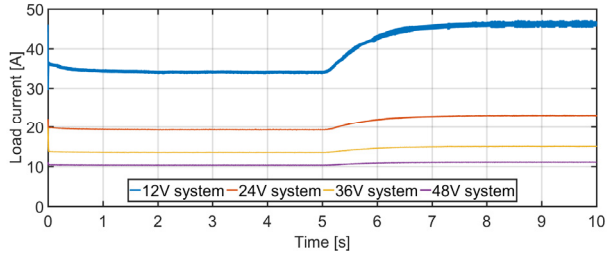

Fig. 15. Load curent for the four cases.

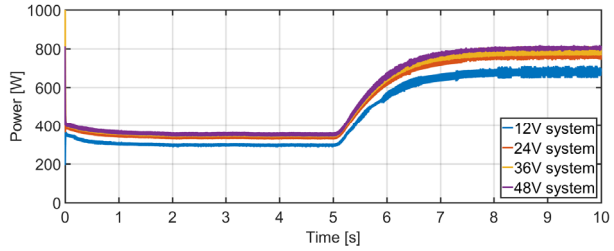

Fig. 16. Comparison of the output power of the NIBB converters.

A. Rectifier Voltage (V_{DC})

The voltage on the output of the diode rectifier behaves in the same manner for all the studied systems - Fig. 8. This behavior is expected, because the rotational speed of the electric generator is the same for the four studied cases and it depends on the turbine operation.

B. Rectifier Current (I_{DC})

The output current of the diode rectifier for two of the studied cases is shown at Fig. 10. This current is composed of rectangular pulses (as it is shown in Fig. 11) due to the principle of operation of the non-inverting buck-boost converter, connected after the rectifier. The amplitude of current pulses is 35A for the 48V system and reaches 80A for the case of 12V battery system. Such high currents could present some problems with the choice of converter components and lead to an increase in the power losses in the system. However, the average output current of the rectifier for all battery voltages is the same because the generator operates under the same conditions. The average output rectifier current in all of the presented cases is under the rated value of 45A.

C. NIBB Converter Output Voltage (V_{NIBB})

The output voltage of the NIBB converter is imposed by the chosen battery configuration. Fig. 12 shows that the voltage stays quite stable. The slight change in the voltage is due to the battery discharge in the period from t=0s to t=5s. After the step in t=5s the battery enters in a charging state which can be seen in the presented results.

D. NIBB Converter Output Current (I_{NIBB})

A comparison of the output currents of the NIBB converters for the studied cases is shown at Fig. 13. As expected the 12V system's current is highest, which sets conditions for higher conduction losses compared to the other studied battery configurations. The excessive current which is produced by the system is stored in the battery for usage in low wind speed conditions.

E. Battery Current (I_{BAT})

The battery currents for the four cases are shown at Fig. 14. The negative values of the current represent battery discharge and the positive values – battery charging state.

The results show that the battery can cover the load needs in low wind speeds and is recharged when the energy production is more than the demand.

F. Load Current (I_{LOAD})

A comparison of the load currents of the four studied cases is presented at Fig. 15. It can be seen that the battery has the ability to provide enough current for the load during low wind speed conditions.

G. Power

The higher currents in the system using 12V battery configuration leads to more conduction losses. This can be seen at Fig. 16, representing a comparison of the converters' output power. This comparison shows that the total power produced diminishes with the output battery voltage. It is notable that the 24V, 36V and 48V systems have significantly better performance concerning the output power compared to the 12V system.

IV. Conclusion

In this paper a low-power wind turbine system with a claw-pole rotor PMSG, non-inverting buck-boost converter and battery energy storage has been studied. A control subsystem including MPPT algorithm and generator power control was attached to the wind turbine system. Mathematical and simulation models in a Matlab environment for all elements operating together were developed. The system was simulated with four different battery voltages and changing wind speed. The simulation results show that the combination of a MPPT algorithm and power control provides good performance and dynamic behavior in following the maximum power of the turbine with relatively simple controller. Besides, it can be concluded that the operation of a variable speed wind turbine with a PMSG is possible with a wide range of battery voltages without any modifications.

The performance of the studied system and the results provide a basis for the optimal choice of battery voltage and capacity, as well as for choosing or designing the appropriate generator for a given wind turbine and output voltage.

Further research can include a study of this system with other types of DC-DC converters (like SEPIC) and its connection to AC grid via an inverter.

Acknowledgment

The research in this publication has been funded the Technical University of Sofia, project 162ПД0010-01.

References

[1] IEC-61400-2:2013, "Wind turbines - Part 2: Small wind turbines".

[2] World Wind Energy Association (WWEA), Small Wind World Report 2016, http://www.wwindea.org/download/small_wind_/SWWR2016-SUMMARYR_2.pdf

[3] K. Buchert and F. W. Fuchs, "Power Losses of Three Phase Rectifier Topologies in Small Wind Turbines," PCIM Europe 2015; International Exhibition and Conference for Power Electronics, Intelligent Motion, Renewable Energy and Energy Management; Proceedings of, Nuremberg, Germany, 2015, pp. 1-8.

[4] V. Lazarov, D. Roye, D. Spirov, "Study of Variable Speed Wind Turbine with Boost and Non-inverting Buck-Boost choppers and Maximum Power control strategy", Japmed'6 Conference, Bucharest, Romania, July 2009.

[5] P. C. Krause, O. Wasynczuk and S. D. Sudhoff. Analysis of electric machinery and drive systems. IEEE Press, Wiley Interscience, 2002.

[6] Z. Zarkov, I. Bachev, B. Demirkov and V. Lazarov, "Experimental Study of Alternator with Permanent Magnets," VIII Science Conference EF 2016, September 12-15, 2016, Varna, Bulgaria.

[7] S. Sivakumar, M. Jagabar Sathik, P.S. Manoj and G. Sundararajan, "An assessment on performance of DC–DC converters for renewable energy applications," Renewable and Sustainable Energy Reviews, 58, 2016, pp. 1475-1485.

[8] M. H. Taghvaee, M. A. M. Radzi, S. M. Moosavain, H. Hizam, and M. H. Marhaban, "A current and future study on non-isolated DC–DC converters for photovoltaic applications," Renewable and Sustainable Energy Reviews, 17, 2013, pp. 216-227.

[9] Z. Tasneem, M. R. I. Sheikh, "Comprehensive modeling and analysis of Variable Speed Wind Turbine using Permanent Magnet Synchronous Generator," 2015 International Conference on Electrical & Electronic Engineering (ICEEE), Rajshahi, 2015, 133-136.

[10] D. Kumar, K. Chatterjee, "A review of conventional and advanced MPPT algorithms for wind energy systems," Renewable and Sustainable Energy Reviews, Vol. 55, March 2016, 957-970.